Biomaterials 119 (2017) 53–67

Contents lists available at ScienceDirect

Biomaterials

journal homepage: www.elsevier.com/locate/biomaterials

Direct induction of neural progenitor cells transiently passes through a partially reprogrammed state

Rui Gao [b, c, 1], Wenchao Xiu [a, 1], Linfeng Zhang [a], Ruge Zang [a], Lei Yang [d], Chenfei Wang [a], Min Wang [e], Mingzhu Wang [a], Li Yi [a], Yuanyuan Tang [d], Yawei Gao [a], Hong Wang [a], Jiajie Xi [a], Wenqiang Liu [a], Yixuan Wang [a], Xuejun Wen [f], Yongchun Yu [e], Yong Zhang [a], Liang Chen [b, c, **], Jiayu Chen [a, *], Shaorong Gao [a, *]

[a] Clinical and Translational Research Center of Shanghai First Maternity & Infant Hospital, School of Life Sciences and Technology, Tongji University, Shanghai, 200092, China
[b] School of Life Sciences, Tsinghua University, Beijing, 100084, China
[c] National Institute of Biological Sciences, NIBS, Beijing, 102206, China
[d] Shanghai First Maternity and Infant Hospital, Tongji University School of Medicine, Shanghai, 200092, China
[e] Institute of Neurobiology, Institutes of Brain Science and State Key Laboratory of Medical Neurobiology, Fudan University, Shanghai, 200032, China
[f] The Institute for Translational Nanomedicine, Shanghai East Hospital, Institute of Biomedical Engineering and Nanoscience, Tongji University School of Medicine, Shanghai, 200092, China

ARTICLE INFO

Article history:
Received 1 November 2016
Received in revised form
7 December 2016
Accepted 7 December 2016
Available online 10 December 2016

Keywords:
Direct induction
giNPCs
Partially reprogrammed state

ABSTRACT

The generation of functional neural progenitor cells (NPCs) holds great promise for both research and clinical applications in neurodegenerative diseases. Traditionally, NPCs are derived from embryonic stem cells (ESCs) and induced pluripotent stem cells (iPSCs), or NPCs can be directly converted from somatic cells by sets of transcription factors or by a combination of chemical cocktails and/or hypoxia. However, the ethical issues of ESCs, the risk of tumorigenesis from iPSCs and transgenic integration from exogenous genes as well as complicated manipulation and time-consuming of chemical induced NPCs (ciNPCs) limit the applications of these strategies. Here, we describe a novel method for generating growth factor-induced neural progenitor cells (giNPCs) from mouse embryonic and adult fibroblasts by using inductive and/or permissive signaling culture conditions. These giNPCs closely resemble brain-derived NPCs in terms of transcription networks and neural lineage differentiation potentials. Moreover, this somatic cell to NPC induction is a gradual process that includes initiation, intermediate, maturation and stabilization stages. Importantly, gene expression and histone modification analyses further indicate a partially reprogrammed state during the generation process of induced NPCs, in which lineage specific genes and pluripotency associated genes are transiently activated. Our study therefore describes the potential safety problems that also exist in the transgene-free direct induction strategy and highlights the importance of excluding the possibility of residual partially reprogrammed and/or teratoma-like cells from the generated NPCs for future clinical trials.

1. Introduction

The generation of induced pluripotent stem cells (iPSCs) [1–3] and induced neuronal cells [4–7] from somatic cells provides not only new cell sources for biomedical research but also potential cell therapy for neurological dysfunction, such as Alzheimer's disease and Parkinson's disease [8–12]. However, the risk of tumorigenicity observed in most iPSC lines may lead to the subsequently differentiated neuronal cells producing certain safety threats [13,14]. On the other hand, the long induction time course, the low efficiency

* Corresponding authors. Clinical and Translational Research Center of Shanghai First Maternity & Infant Hospital, School of Life Sciences and Technology, Tongji University, Shanghai, 200092, China.
** Corresponding author. National Institute of Biological Sciences, NIBS, Beijing, 102206, China.
E-mail addresses: chenliang@nibs.ac.cn (L. Chen), chenjiayu@tongji.edu.cn (J. Chen), gaoshaorong@tongji.edu.cn (S. Gao).
[1] These authors contributed equally to this work.

http://dx.doi.org/10.1016/j.biomaterials.2016.12.007
0142-9612/

and the restricted proliferative potential of induced differentiated neuronal cells limit the clinical applications of this strategy. By contrast, induced neural progenitor cells (iNPCs), which are capable of self-renewing and differentiating into a wide range of neural cell lineages, hold great promise for therapeutic approaches [15,16]. Currently, diverse mouse [17–22] and human [23] cell types have been successfully converted to iNPCs via different direct induction strategies with the overexpression of transcription factors in various combinations. These direct conversion approaches proved to be highly efficient and time-saving, but the risk of genomic integration of the viral vectors sustains debates regarding safety. Alternatively, a footprint-free strategy for reprograming human urine epithelial-like cells into NPCs using an episomal system has been established [24]. More recently, an important advance has indicated that small molecules can be used to generate chemical-induced neural progenitor cells (ciNPCs) from somatic cells without introducing exogenous genes [25,26]. This new means of induction has considerable advantages because the small molecules are nonimmunogenic and cost-effective. Moreover, their effects on activating and inhibiting the function of specific factors are reversible and can be finely modulated by adjusting their concentrations. However, this direct induction strategy involves complicated and replicated manipulation of chemical cocktails and a strict physiological hypoxic condition [25].

Previously, direct conversion at the molecular level was typically achieved by ectopic expression of sets of cell type-specific transcription factors [27,28]. However, a more general lineage conversion approach is to transiently overexpress the conventional Yamanaka factors [17,19,29,30]. This strategy suggested that the transient expression of pluripotency-associated genes could generate a plastic intermediate state, which further serves as a cellular platform for transdifferentiation into various lineages in the presence of lineage-specifying extracellular signaling inputs. These processes did not involve the establishment of a pluripotent state because mouse somatic cells subjected to Yamanaka-factor-based conversion approaches failed to activate transgenic pluripotent reporters such as *Oct4*-GFP [17,19]. However, two recent independent studies using different lineage tracing systems conflicted with these issues [31,32]. The studies both concluded that transdifferentiation systems using pulsed expression of pluripotency-associated factors in combination with differentiation-inducing signals indeed involved a short-lived Oct4-positive iPSC-like state. Then, the cells rapidly differentiated into the specified lineages [31,32]. Notably, passage through a transient pluripotent state might be the result of using pluripotency-associated transcription factors. Thus, our interests arose from two unsolved issues regarding: 1) Whether external inductive and/or permissive signaling culture conditions could induced neural progenitor cells from somatic cells? 2) If the direct cell type switch from somatic cells to functional NPCs without introducing exogenous genes also involves a similar transient stage? Answering these questions will increase our understanding of the molecular mechanism underlying the establishment of induced neural progenitor cells. Further, answering these questions will provide safety verification information for generating functionally desirable cell types with potential regenerative applications by cell fate reprogramming using specific growth factors or chemical compounds instead of genetic manipulation.

Here, we present a novel method for generating growth factor-induced neural progenitor cells (giNPCs) by using inductive and permissive signaling culture conditions with the combination of only a few growth factors. We show that these giNPCs are very similar to neonatal mouse brain-derived NPCs in terms of transcription networks and neural lineage differentiation potential *in vivo* and *in vitro*. We demonstrate that somatic cell to NPC induction is a gradual process that includes initiation, intermediate, maturation and stabilization stages with the erasure of a somatic-specific platform and establishment of an NPC-specific network. Importantly, our data further suggest that both our giNPC and previously reported ciNPC induction go through a partially reprogrammed state in which lineage genes from three germ layers and pluripotency-associated genes are transiently activated with the corresponding reconstitution of histone modifications.

2. Materials and methods

2.1. Mouse and cell culture

The specific pathogen-free mice were housed in the animal facility of Tongji University. All our study procedures were consistent with the Tongji University Guide for the care and use of laboratory animals. Mouse embryonic fibroblasts (MEFs) were isolated from 13.5-dpc embryos. Tail-tip fibroblasts (TTFs) were isolated from the adult Nestin-GFP transgenic mice. MEFs and mouse TTFs were maintained in somatic cell culture medium [DMEM (Life Technologies) supplemented with 10% (vol/vol) FBS (Gibco) and 1 mM L-glutamine (Merck Millipore)] at 37 °C with 5% CO_2. Mouse brain-neural progenitor cells (Brain-NPCs) were derived from neonatal mice, digested by Accutase (Sigma) and cultured in NPC expansion medium [DMEM/F12 supplemented with 1% N2 (Invitrogen) and 2% B27 (Invitrogen), 20 ng/mL basic fibroblast growth factor (bFGF; R&D Systems) and 10 ng/mL epidermal growth factor (EGF; Peprotech)], as previously described [33].

2.2. Generation of giNPCs

For induction of neural progenitor cells, 1.5–2 × 10^5 MEFs or TTFs were initially plated in a well of a 24-well plate in initiation medium [DMEM/F12 with the following supplements: 1% GlutaMAX (Gibco), 2% B27 minus vitamin A (Gibco), 1 μg/mL heparin (Stem Cell Technologies), 1000 units/mL LIF (Merck Millipore), 20 ng/mL bFGF and 20 ng/mL EGF]. Cells were gently pipetted each day for the first week to prevent them from attaching to the dish bottom and to generate good sphere formation. After two weeks, the cells were digested by trypsin/EDTA (Invitrogen) and expanded to a 12-well or a 35-mm tissue culture dish in the presence of NPC expansion medium. For MEF-giNPC induction, 7 days later, the neural rosettes were pipetted and passaged in suspension onto ultralow attachment plates (Costar) to form the growth factor-induced neural progenitor cells. For TTF-giNPC induction, the neural rosettes were pipetted and passaged in suspension after 2 weeks. These formed MEF-giNPCs or TTF-giNPCs were cultured in suspension or under single-cell monolayer conditions for 3–4 rounds of passaging to select for the fully induced giNPCs. During the giNPC induction process, the culture medium was partially changed every other day.

2.3. Generation of ciNPCs

The chemical induced neural progenitor cells (ciNPCs) were generated as previously reported [25]. Briefly, initial 2 × 10^5 MEFs were seeded in each well of 6-well plates in KSR medium with chemical compounds (0.5 mM VPA, 3 μM CHIR99021, 1 μM Repsox and 2 μM Parnate). As indicated previously [25], VPA is an HDAC inhibitor and Parnate is an H3K4 demethylation inhibitor. The effects of these two small molecules suggest that H3K4 demethylation and histone deacetylation could be two critical epigenetic barriers to reprogramming. CHIR99021 is a GSK3-β inhibitor and Repsox is a TGF-β signaling inhibitor. Either of them could efficiently replace Sox2 for reprogramming. Cells were cultured at

37 °C under 5% O_2 (hypoxia) and 5% CO_2. Medium containing chemical compounds was changed every other day. 10 days later, cell mixtures were digested by trypsin/EDTA and expanded in NPC expansion medium under 20% O_2 (normoxic) conditions. ciNPCs were formed around day 20 and were enriched by rounds of neurosphere suspension culture.

2.4. In vitro differentiation of giNPCs

For spontaneous differentiation into all neural types, 5×10^4 giNPCs were plated onto PDL (Invitrogen)/Laminin (Sigma)-coated glass coverslips in 12 wells containing NPC expansion medium. After 24 h, the medium was switched to NPC expansion medium without growth factors for 1–2 weeks [23]. Robust astrogenesis was induced by adding 1% FBS to NPC expansion medium without growth factors for one week [23]. For the analysis of the neuronal differentiation potential of the giNPCs, the cells were plated onto PDL/Laminin-coated glass coverslips in 12 wells in medium consisting of a 1:3 mix of DMEM/F12 and Neurobasal (Invitrogen), 1% N2 and 2% B27 supplements, and 6.7 ng/mL bFGF and 20 ng/mL brain-derived neurotrophic factor (BDNF; PeproTech). After 3 days, the media was replaced with fresh medium with a reduced amount of 5 ng/mL bFGF and an increased amount of 30 ng/mL BDNF. The cells were maintained under these conditions for an additional 10–15 days, and the medium was partially changed every 2–3 days [34,35]. For oligodendrocyte differentiation, the cells were plated onto PDL/Laminin-coated coverslips and cultured in N2B27 medium with 10 ng/mL bFGF and 10 ng/mL PDGF-AA (Peprotech) for 3 days and then with 100 ng/mL T3 (Sigma-Aldrich) for 4–6 days [36].

2.5. RNA preparation and quantitative real-time PCR

Total RNA was extracted using Trizol reagent (Invitrogen) and reverse transcribed using 5X All-in-One RT MasterMix (Applied Biological Materials) according to the manufacturer's recommendations. Quantitative RT-PCR was performed using SYBR Premix Ex Taq II (Takara), and the signals were detected with an ABI7500 Real-Time PCR System (Applied BioSystems). All samples were run in triplicate. Glyceraldehyde 3-phosphate dehydrogenase (*Gapdh*) was used as an endogenous control. The values were normalized based on *Gapdh* expression. All the primers used were synthesized at SangonBiotech (Shanghai) Co., Ltd, and are listed in Table S1.

2.6. Confocal microscopy, immunofluorescent staining and quantitative analyses

For immunofluorescent staining, MEFs, mouse TTFs, giNPCs, Brain-NPCs or neural cells were plated onto PDL-coated glass coverslips (Thermo). The cells were fixed in 4% paraformaldehyde (Sigma) overnight at 4 °C. After washing in phosphate buffered saline (PBS), the cells were permeabilized for 15 min in PBS containing 0.5% Triton X-100 and, subsequently, were blocked with 2.5% bovine serum albumin (BSA) in PBS for 1 h at room temperature. Then, the cells were incubated overnight at 4 °C in PBS containing 2.5% BSA with the primary antibodies. The primary antibodies used in this study were as follows: mouse anti-Nestin (1:1000; Chemicon), goat anti-Sox1 (1:1000, R&D Systems), mouse anti-Sox2 (1:500; Santa Cruz Biotechnology), rabbit anti-β-III-Tubulin (Tuj1, 1:1000; Covance), mouse anti-Map2 (1:500; Millipore), and rabbit anti-Gfap (1:1000; Millipore). Then, the cells were washed three times with PBS and incubated for 1 h at room temperature with secondary antibodies conjugated with Alexa-Fluor 488, AlexaFluor 594, or AlexaFluor 633 (1:500; Invitrogen). The DNA was labeled with 4′, 6-diamidino-2-phenylindole (DAPI). The glass coverslips were observed with a NIKON ECLIPSE 80i microscope or ZEISS LSM 880 microscope using the Plan Fluor 20X or 40X DIC or 63X Oil objective.

For quantitative analyses of giNPCs' differentiation efficiency, giNPCs were plated onto PDL/Laminin-coated glass coverslips in 12-well plates containing certain differentiation medium. MEFs and Brain-NPCs were set as negative and positive controls, respectively. In order to exclude mutual interference between primary antibodies, each coverslip was stained with only one primary antibody. Three independent experimental replicates were conducted. For each immunostaining experiment, three vision fields of one kind of differentiation were randomly selected. The “Percentage (%)” was calculated as the total marker positive cells (immunoreactive cells) over total DAPI positive cells. The actual number of cells showing immunoreactivity for each marker as well as the whole population under certain differentiation conditions are provided in Table S2.

2.7. Electrophysiological analysis

Electrophysiological experiments were performed using giNPC 1#- or Brain-NPC-derived neurons. Whole-cell patch clamp recordings in either voltage or current clamp mode were conducted to measure voltage-activated sodium/potassium currents and action potentials. The output signals from the Multiclamp 700B amplifier were digitized using a DigiData 1440 A/D D/A board, low-pass filtered at 5 KHz. Glass micropipettes (2.0–4.0 MΩ) containing a solution of 130 mM K^+-gluconate, 20 mM KCl, 10 mM HEPES, 0.2 mM EGTA, 4 mM Mg_2ATP, 0.3 mM Na_2GTP, and 10 mM Na^{2+}-phosphocreatine (at pH 7.3, 290–310 mOsm) were used for patch-clamp recordings. The bath solution contained 140 mM NaCl, 5 mM KCl, 2 mM $CaCl_2$, 2 mM $MgCl_2$, 10 mM HEPES and 10 mM glucose (at pH 7.4). Membrane potentials were hold around −100 mV, and step currents with an increment of 20 pA were injected to elicit action potentials. A ramp protocol (from −80 to +60 mV) was used to elicit inward sodium current and outward potassium currents. Data were analyzed using pClamp10 (Clampft).

2.8. In vivo transplantation

In vivo transplantation was performed as previously described [37]. Briefly, uterine horns of E13.5 gestation stage pregnant C57BL/6 mice were maintained in pathogen-free condition. 2 μl PBS containing around 20 GFP-giNPC line 1# neurospheres with neurosphere diameter less than 80 μm was injected into the embryonic cerebral ventricle through a bevelled, calibrated glass micropipette. After that, the uterine horns were replaced, the peritoneal cavity was lavaged with 10 mL warm PBS containing antibiotics and the wound was closed. 1 month after birth, mice were anesthetized on ice or with pentobarbital sodium and brains section were prepared as described above for further analysis. The primary antibodies used in the following study were as follows: mouse anti-GFP (1:100; Proteintech) and rabbit anti-β-III-Tubulin (Tuj1, 1:1000; Covance). The brains section were observed with a Zeiss LSM 880 with airyscan microscope using the Plan Fluor 25X or 63X Oil objective.

2.9. Teratoma assay and H&E staining

A total of 5×10^5 cells, including the induction cells from Day 0, Day 1, Day 4, Day 7, Day 10, and Day 14 as well as giNPC (lines 1# and 2#), brain-NPCs and iPSCs, were individually suspended in 250 μl of PBS and subcutaneously injected into the SCID mouse to test their teratoma formation ability. Four weeks post-injection, subcutaneous tissue were dissected and processed for

hematoxylin-eosin (H&E) staining, which was performed at the Shanghai Yichang Biological Technology Co., Ltd.

2.10. RNA-seq library generation and illumina HiSeq 2500 sequencing

During the giNPC induction process, cell samples were harvested at various induction days including Day 1, Day 4, Day 7, Day 10, Day 14, Day 17 and Day 21. Simultaneously, samples from primary neurosphere-like cluster (pre-NPCs), an established giNPC cell line at passage 6 (giNPCs P6), Brain-NPCs as well as teratoma cells were also collected. Total RNA was isolated from cell pellets using Trizol reagent, and RNA-seq libraries were generated using KAPA Stranded mRNA-Seq Kits according to the manufacturer's recommendations. Briefly, the mRNA was enriched using oligo (dT) magnetic beads and sheared to create short fragments of approximately 300 bp. cDNA was synthesized using random hexamer primers and purified using 1.8X Agencourt AMPure XP beads (Beckman). Finally, the sequencing primers linked to the cDNA fragments (approximately 300 bp) were isolated by gel electrophoresis and enriched by PCR amplification to construct the library. The sequencing was performed at the Berry Genomics Co Ltd. and the Sequencing Center in National Institute of Biological Sciences, Beijing, using the HiSeq 2500 system developed by Illumina. Paired-end sequencing was applied.

2.11. Sequencing analysis

Public RNA-seq datasets including MEFs (GSE43986), mouse ESCs (GSE59463) and iPSCs (GSE54619) were downloaded from the GEO data repository and integrated in the analysis. All RNA-seq reads were mapped to the mouse genome using the Tophat software (version: v2.0.12) [38]. The expression level for each gene was quantified to the reads count using htseq-count software (version: 0.6.0) and to FPKM using Cufflinks software (version: v2.2.1) [39]. Then, the clustering analysis was performed by heatmap and PCA packages within custom R script software. Differential expression analysis was conducted using edgeR software (version: 3.12.0) on the basis of a comprehensive consideration of the P value (cutoff to 0.05) and fold-change (cutoff to 4.5) via the 'Cuffdiff' command [40].

2.12. Chromatin immunoprecipitation (ChIP)

ChIP experiments were performed using the MAGnify™ Chromatin Immunoprecipitation System (Invitrogen) according to the manufacturer's recommendations. Briefly, ~10^5 cells were resuspended in lysis buffer, and chromatin was sonicated to 200–500 bp with the Covaris M220 system. Then, the sonicated chromatin was immunoprecipitated with the following antibodies: anti-H3K4me3 (Abcam) and anti-H3K27me3 (Millipore). A fraction of 'whole-cell extract' obtained without antibody was retained as an input control, whereas DNA fragments obtained with normal rabbit or mouse IgG were applied as negative controls. The DNA isolated from the ChIP was quantified using a Qubit 2.0 Fluorometer (Life Technologies), and qRT-PCR was performed to validate the enrichment amounts. The primers are listed in Table S1.

2.13. Statistics

The Holm-Sidak test (for ANOVA) or Student's test was performed using GraphPad Prism 5 software for statistics comparison.

2.14. Accession numbers

The RNA-seq datasets have been deposited in Gene Expression Omnibus (GEO) and are accessible under the GEO accession number GSE76857.

3. Results

3.1. Growth factor induction of mouse neural progenitor cells (NPCs)

Previous studies provided evidence that direct lineage conversion of different somatic cells to self-renewal, multipotent and neural lineage-restricted NPCs could be achieved by sets of defined transcription factors [17–23] or by using the combination of chemical cocktails and/or hypoxia [25,26]. However, due to the introduction of exogenous genes as well as the complicated manipulation of chemicals, there are still a lot of concerns coming along these techniques. Here, we presented a novel method using inductive and permissive signaling culture conditions with the combination of only a few growth factors including B27 minus vitamin A, heparin, LIF, bFGF and EGF, which could successfully induce NPCs from differentiated somatic cells. Firstly, mouse embryonic fibroblasts (MEFs) were plated and cultured in the initiation medium with the following supplements: B27 minus vitamin A, heparin, LIF, bFGF and EGF. Cells were gently pipetted each day for the first week to prevent them from attaching to the dish bottom, and sphere morphology was visualized (Fig. 1A and B, Day 1 and Day 7). Secondly, these sphere-like colonies attached to the bottom of the culture dishes, followed by cell mixtures migrating and gradually forming monolayer structures in the following week (Fig. 1A and B, Day 14). Thirdly, cell mixtures were digested and expanded in the presence of NPC expansion medium with the following supplements: N2, B27, bFGF and EGF (Fig. 1A and B, Day 15) to establish primary neurosphere-like networks (Fig. 1A and B, Day 21). Lastly, primary NPC-like cells (Fig. 1A and B, Pre-NPCs) were isolated and subjected to 3–4 rounds of passaging to select for the fully induced neural progenitor cells (giNPCs). Free-floating clusters were observed when these giNPCs were cultured in suspension (Fig. 1A and B, giNPCs in suspension). Alternatively, under single-cell monolayer culture conditions, NPC-like bipolar morphology was observed (Fig. 1A and B, adherent giNPCs). In addition, the flow cytometric analysis and imaging of this growth factor mediated induction process by using Nestin-GFP MEF cells further indicated a gradual acquisition of the neural phenotype (Fig. 1C–D and S1A-S1B). Simultaneously, we verified the extent of cell death and cell viability during this process. Early apoptosis under the long induction period displayed many minor fluctuations, whereas the extent of late apoptosis and cell death gradually decreased (Fig. S1C). Overall, the extent of cell death under the growth factor mediated induction process is not significant.

3.2. giNPCs show transcriptional profiles similar to those of brain-NPCs

To characterize the identity of growth factor-induced NPCs (giNPCs), we performed comprehensive molecular analysis at the transcription and protein levels. We randomly chose four giNPC lines, which were derived from several independent experimental replicates and were cultured in suspension (giNPC lines 1# and 2#) or adherent (giNPC lines 5# and 6#) culture conditions. All giNPCs displayed typical NPC morphologies (Fig. 1B, giNPCs in suspension and adherent giNPCs), and the mean doubling times were similar to that of brain-derived NPCs (Brain-NPCs) (Fig. S2A). Quantitative analysis demonstrated that giNPCs expressed typical NPC markers,

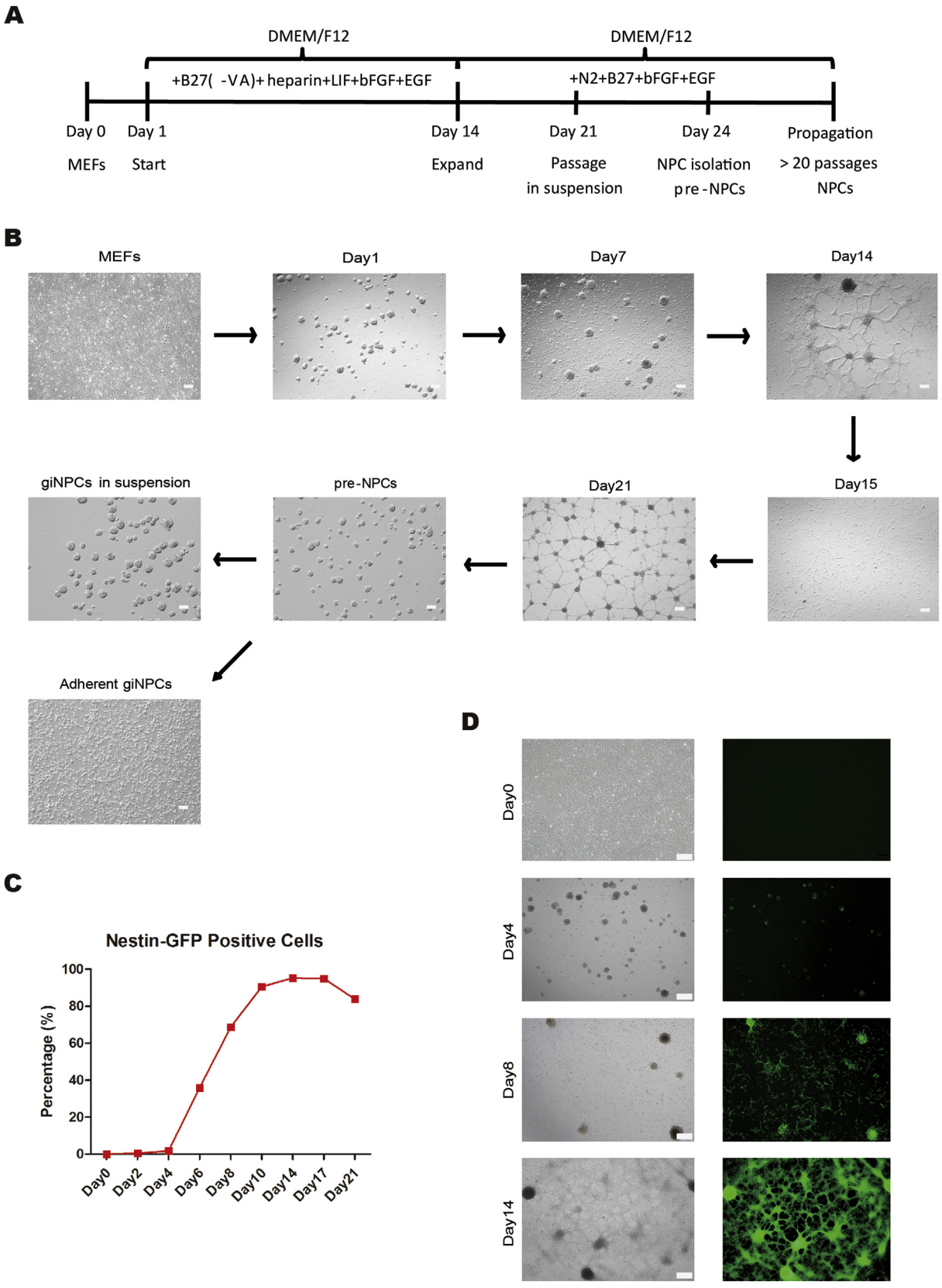

Fig. 1. Growth Factor induction of mouse NPCs. (A) Strategy for induction of giNPCs from mouse embryonic fibroblasts (MEFs). 1.5–2 × 10^5 MEFs were plated and cultured in the initiation medium with the following supplements: B27 minus vitamin A, heparin, LIF, bFGF and EGF. Cells were gently pipetted each day for the first week to prevent them from attaching to the dish bottom. After two weeks, the cells were digested and expanded to a 12-well or a 35-mm tissue culture dish in the presence of NPC expansion medium with the following supplements: N2, B27, bFGF and EGF. 7 days later, the neural rosettes were pipetted and passaged in suspension onto ultralow attachment plates to form the growth factor-induced neural progenitor cells (giNPCs). (B) Morphological changes of cells during the induction process at indicated time points. Scale bar, 200 μm. At the first week, MEFs were induced by the initiation medium, and sphere morphology was observed. During the following week, these sphere-like colonies attached to the bottom of the culture dishes, cell mixtures migrated and the monolayer structure appeared. Then, cell mixtures were digested at Day14 and expanded in the presence of NPC expansion medium to form primary neurosphere-like networks. Finally, fully induced giNPCs could be generated and propagated after 3–4 rounds of passages under suspension or monolayer culture conditions. (C) The kinetics of giNPC induction from Nestin-GFP MEF cells showed a gradual acquisition of GFP positive signals. (D) Representative images of cells during the induction process from Nestin-GFP MEF cells at indicated time points. Scale bar, 200 μm.

including *Nestin*, *Pax6* and *Sox2*, instead of fibroblast-associated genes *Thy1* and *Col3a1*, which was similar to the expression of Brain-NPCs (Fig. 2A and S2B). Immunofluorescent staining further confirmed that giNPCs, like Brian-NPCs, were consistently positive for NPC markers, including Nestin, Sox2 and Sox1 (Fig. 2B and S2C). However, no morphological changes or Nestin-, Sox1-, or Sox2-

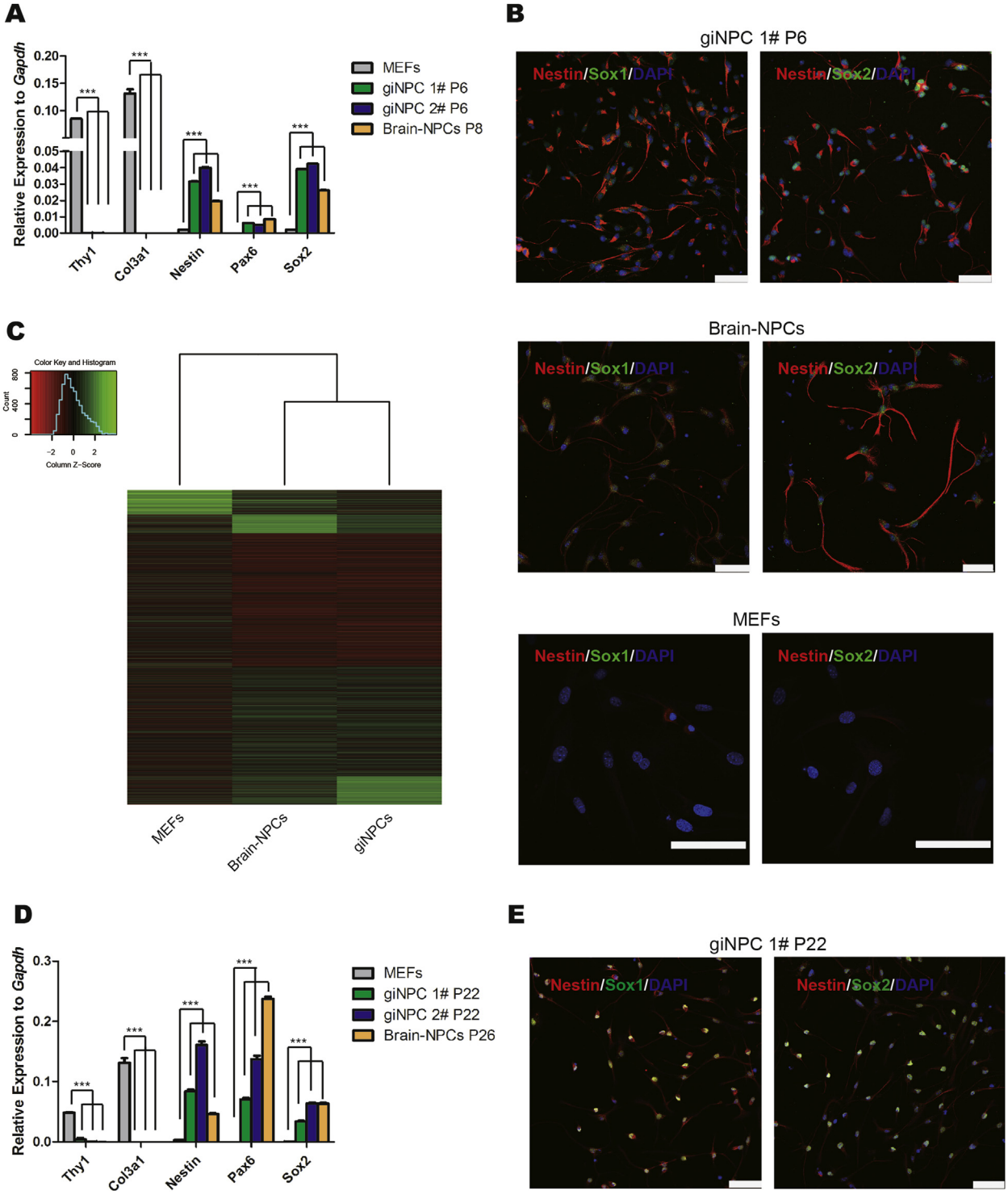

Fig. 2. Characterization of giNPCs. (A) qRT-PCR analysis of fibroblast- and NPC- specific genes in giNPC lines 1# and 2# at passage 6. giNPC lines 1# and 2# are suspended and cultured in NPC expansion medium. Brain-NPCs (passage 6) and MEFs are set as controls. The expression levels were normalized to *Gapdh*. (B) Immunofluorescent staining of NPC specific markers in giNPC line 1# at passage 6. These giNPCs are subjected to monolayer culture. Brain-NPCs and MEFs are positive and negative controls, respectively. Scale bar, 50 μm. (C) Heatmap and hierarchical clustering of gene expression profiles in giNPCs, Brain-NPCs and MEFs. (D) qRT-PCR analysis of fibroblast- and NPC- specific genes in giNPC lines 1# and 2# at passage 22. Brain-NPCs (passage 26) and MEFs are set as controls. The expression levels were normalized to *Gapdh*. (E) Immunofluorescent staining of NPC specific markers in giNPC line 1# at passage 22. These giNPCs are subjected to monolayer culture. Scale bar, 50 μm. Data in (A) and (D) are represented as the mean ± SEM (n = 3). ***$p < 0.001$ by ANOVA or Student's *t*-test for comparison.

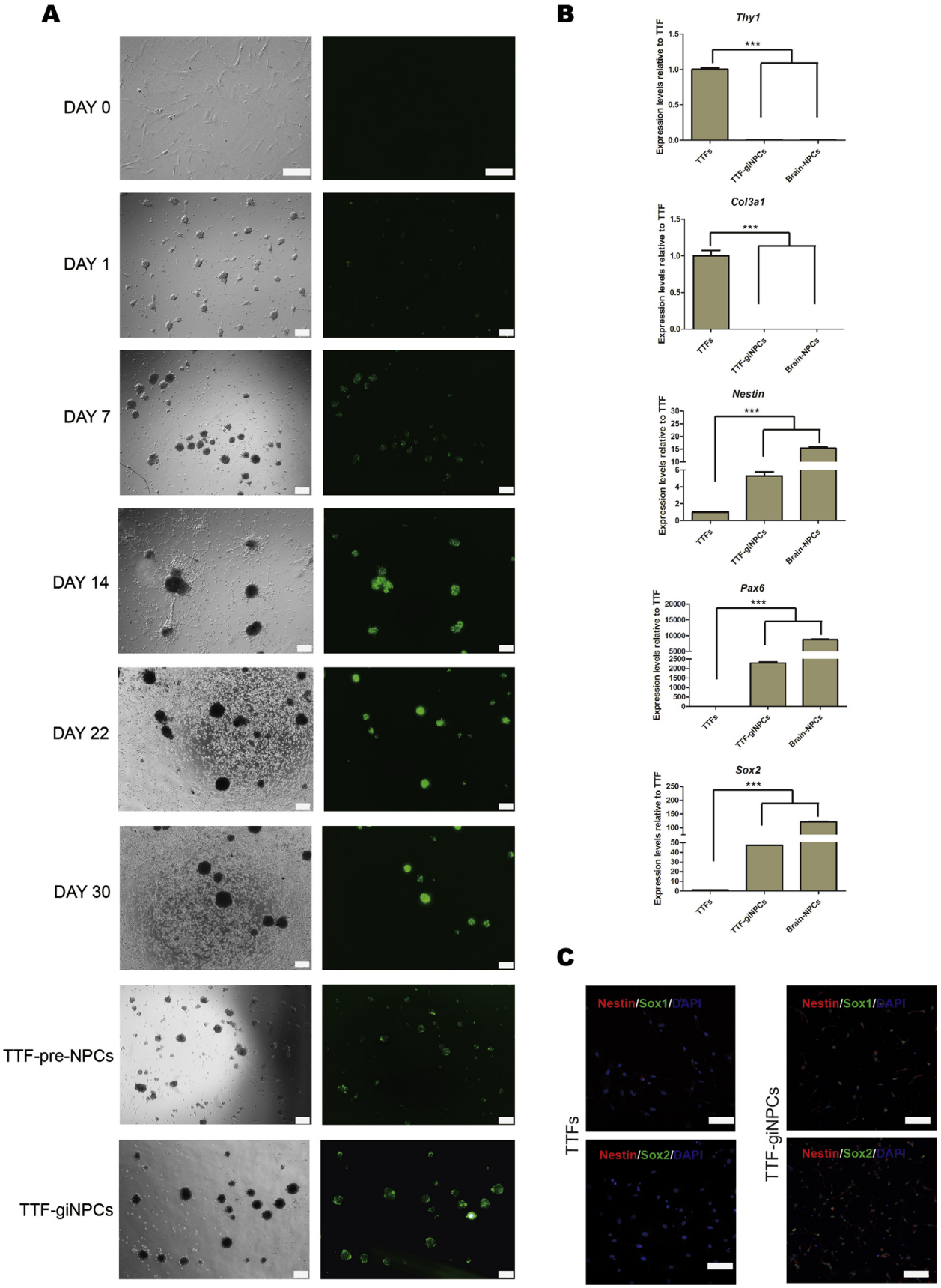

Fig. 3. Generation of giNPCs from mouse adult fibroblasts. (A) Morphological changes of cells during the induction process at indicated time points. Tail-tip fibroblasts (TTFs) were derived from Nestin-GFP transgenic mice. No Nestin-GFP positive cells were observed in the starting TTFs, while Nestin-GFP positive and neurosphere-like cells gradually appeared. Nestin-GFP positive TTF-giNPCs were then generated. Scale bar, 200 μm. (B) qRT-PCR analysis of fibroblast- and NPC-specific gene expression in TTF-giNPCs. Brain-NPCs and TTFs are set as controls. The expression levels were normalized toTTF. (C) Immunofluorescent staining of NPC specific markers in TTF-giNPCs. Brain-NPCs and TTFs are positive and negative controls, respectively. Scale bar, 100 μm. Data in (B) are represented as the mean ± SEM (n = 3). ***$p < 0.001$ by Student's *t*-test for comparison.

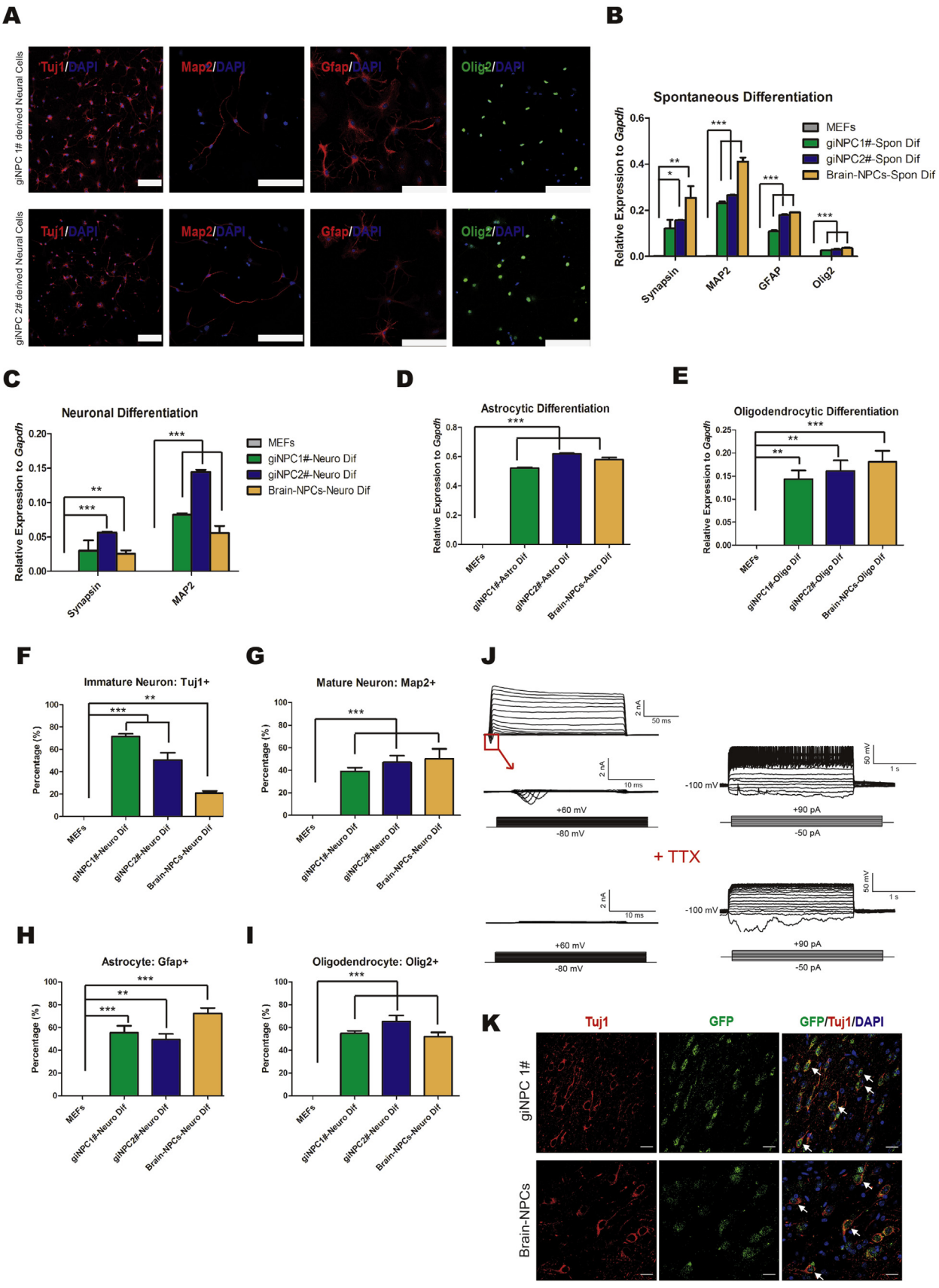

Fig. 4. giNPCs can differentiate into neural lineages. (A) Immunofluorescent staining of differentiation markers Tuj1 (neurons), Map2 (mature neurons), Gfap (astrocytes) and Olig2 (oligodendrocytes) in neuronal cells derived from giNPCs. Scale bar, 25 μm. (B–E) qRT-PCR analysis of indicated markers in spontaneous differentiated cells (A), neurons (B),

positive cells were observed when MEFs were cultured in somatic cell culture medium (Fig. 2B). Importantly, the global gene expression profiles of giNPCs resembled Brain-NPCs but were quite distinct from those of MEFs (Fig. 2C and S2D). Moreover, these giNPCs maintained the NPC characteristics after prolonged culture in their morphologies, proliferation potency or gene expression (Fig. 2D–E and S2E-S2F). Taken together, these data suggest that homogenous expandable giNPCs resembling Brain-NPC properties can be successfully generated from MEFs in our system.

3.3. Generation of giNPCs from adult mouse fibroblasts

To rule out the possibility that giNPCs were induced from certain neural cell types in the starting MEF populations, we treated tail-tip fibroblasts (TTFs) from adult Nestin-GFP transgenic mice in the same induction system. No Nestin-GFP positive cells were observed in the starting TTFs, whereas during the induction process, Nestin-GFP positive cells appeared at an early stage, and the GFP signaling gradually increased (Fig. 3A). In all, the morphological changes in giNPCs induced from TTFs were similar to those from MEFs, and mature TTF-giNPCs were successfully obtained despite a prolonged induction period. These Nestin-GFP positive TTF-giNPCs had typical NPC morphology and neurosphere-forming ability. The qRT-PCR and immunostaining analyses further confirmed that TTF-giNPCs expressed NPC markers, including *Nestin*, *Pax6* and *Sox2*, as Brain-NPCs did (Fig. 3B and C). However, *Thy1* and *Col3a1*, the fibroblast specific genes, were down-regulated (Fig. 3B). Moreover, no NPC-specific markers were expressed in the starting TTFs (Fig. 3B and C). In conclusion, giNPCs can be induced not only from mouse embryonic fibroblasts but also from mouse adult fibroblasts.

3.4. giNPCs can differentiate into neural lineages

We then analyzed the developmental potential of giNPCs by assessing their capacity for differentiation into the major subtypes of the neural lineage. By removing growth factors from the NPC expansion medium for 1–2 weeks, giNPCs were able to differentiate into neurons (Tuj1-positive or Map2-positive) or astrocytes (Gfap-positive), which were similar to Brain-NPCs (Fig. 4A–B and S3A). For mature neuronal differentiation, the differentiated cells from giNPCs showed typical neuronal morphology and expressed neuronal cell markers *Map2* and *Synapsin* (Fig. 4A and C). Moreover, these cells displayed expression of glutamatergic and GABAergic neuron markers, which indicated mature synapse formation (Fig. S3B and S3D). Quantitative analysis of the immunostaining results further showed that efficiency of glutamatergic differentiation between giNPCs and Brain-NPCs were comparable (Fig. S3C). Besides, giNPCs could also differentiate into astrocytes (Gfap–-positive) and oligodendrocytes (Olig2-positive) as Brain-NPCs did (Fig. 4A and D-E). In addition, quantitative analysis demonstrated that the *in vitro* differentiation efficiencies of giNPCs into major neural lineages was quite similar to those of Brain-NPCs (Fig. 4F–I). In contrast, the starting MEFs did not express neuronal cell markers, which was quite different from cells differentiated from giNPCs (Fig. 4A–I and S3A-S3C).

The maturity and function of giNPCs were further assessed by *in vitro* and *in vivo* analyses. By whole-cell patch-clamp analysis, the differentiated neurons from giNPCs, similar to those differentiated from Brain-NPCs, expressed voltage-gated ion channels and had the ability to generate single or multiple action potentials evoked by current injection, indicating functional membrane properties (Fig. 4J and S3E). Thus, giNPCs are capable of differentiating into major neural lineages *in vitro*, which are quite similar to their counterparts derived from newborn brain tissue. To determine the giNPC's developmental potential *in vivo*, giNPCs were microinjected into the embryonic cerebral ventricle of E13.5 pups, and their survival and differentiation were evaluated about 1 month after these pups were born [37]. Remarkably, neither obvious developmental abnormality nor tumors or deformity was observed in these transplanted pups. Further immunofluorescent analysis demonstrated that cells differentiated from transplanted giNPCs were able to survive and migrate into diverse brain sections, which closely resembled Brain-NPCs (Fig. 4K).

3.5. Induction of giNPCs is a gradual process

To gain insight into the molecular mechanisms involved in the giNPC induction process, we harvested samples at different time points and compared the global gene expression profiles of these cells by RNA-seq analysis. The global genome heatmap indicated a genome-wide transcriptional conversion from a somatic state to an NPC state (Fig. S4A). Accordingly, both principal component analysis (PCA) and unsupervised hierarchical clustering analysis indicated that this somatic to NPC induction was a gradual process, which included the initiation, intermediate, maturation and stabilization stages (Fig. 5A and B). At the initiation stage, MEFs were induced by the initiation medium, and sphere morphology was observed within the first week (Fig. 1B and 5A-B, Day 1, Day 4 and Day 7). At the intermediate stage, the monolayer structure appeared, and cells started to express NPC specific genes (Fig. 1B and 5A-B, Day 10 and Day 14). Surprisingly, cells in this stage showed a transcriptional profile similar to that of teratomas, which are known to express genes from three germ layers. At the maturation stage, primary neurosphere-like networks formed, and NPC specific genes were prominently up-regulated (Fig. 1B and 5A-B, Day 17 and Day 21). At the stabilization stage, free floating giNPCs could be generated and propagated after 3–4 rounds of passages, showing a transcriptional pattern similar to that of Brain-NPCs (Fig. 1B and 5A-B). These various transcriptional patterns were further confirmed by hierarchical clustering and Pearson analysis, which demonstrated that the global gene expression patterns of giNPCs were similar to those of brain-NPCs but were different from those of ESCs, iPSCs and MEFs (Fig. 5C).

3.6. Transcriptome dynamics in the direct induction system

Based on the gene-expression dynamics, we clustered the significantly changed genes into eight groups (3106 genes in total) during the giNPC induction process (Fig. 6A). A large set of genes (clusters I, II, III and IV) including fibroblast markers were repressed across this process. Meanwhile, previously reported Mesenchymal-to-Epithelial Transition (MET) associated genes, such as *Thy1*, *Col1a1* as well as *Col3a1*, were included (Fig. 6A, clusters II and III and Figs. S4B–S4C) [41]. By contrast, neural specific markers, such

astrocytes (C) and oligodendrocytes (D) derived from giNPCs. MEFs and neuronal cells derived from Brain-NPCs are negative and positive controls, respectively. The expression levels were normalized to *Gapdh*. (F–I) Quantitative analysis of indicated immature neurons (F), mature neurons (G), astrocytes (H) and oligodendrocytes (I) obtained following giNPC differentiation. MEFs and neuronal cells derived from Brain-NPCs are set as negative and positive controls, respectively. (J) Electrophysiological properties of functional neurons differentiated from giNPC line 1#. Whole cell recordings show voltage-gated currents and evoked action potentials in response to the injected current. Simultaneously, inward currents can be blocked by adding tetrodotoxin (TTX). (K) Immunostaining of *in vivo* transplanted GFP labeled giNPC line 1#. The transplanted brain-NPCs are set as the control. Arrows indicate GFP + cells expressing Tuj1. Nuclei were counterstained with DAPI. Scale bar, 20 μm. Data in (B)–(E) are represented as the mean ± SEM (n = 3). Data in (F)–(I) are represented as the mean ± SEM (n = 9). $^{*}p < 0.05$; $^{**}p < 0.01$; $^{***}p < 0.001$ by ANOVA or Student's *t*-test for comparison.

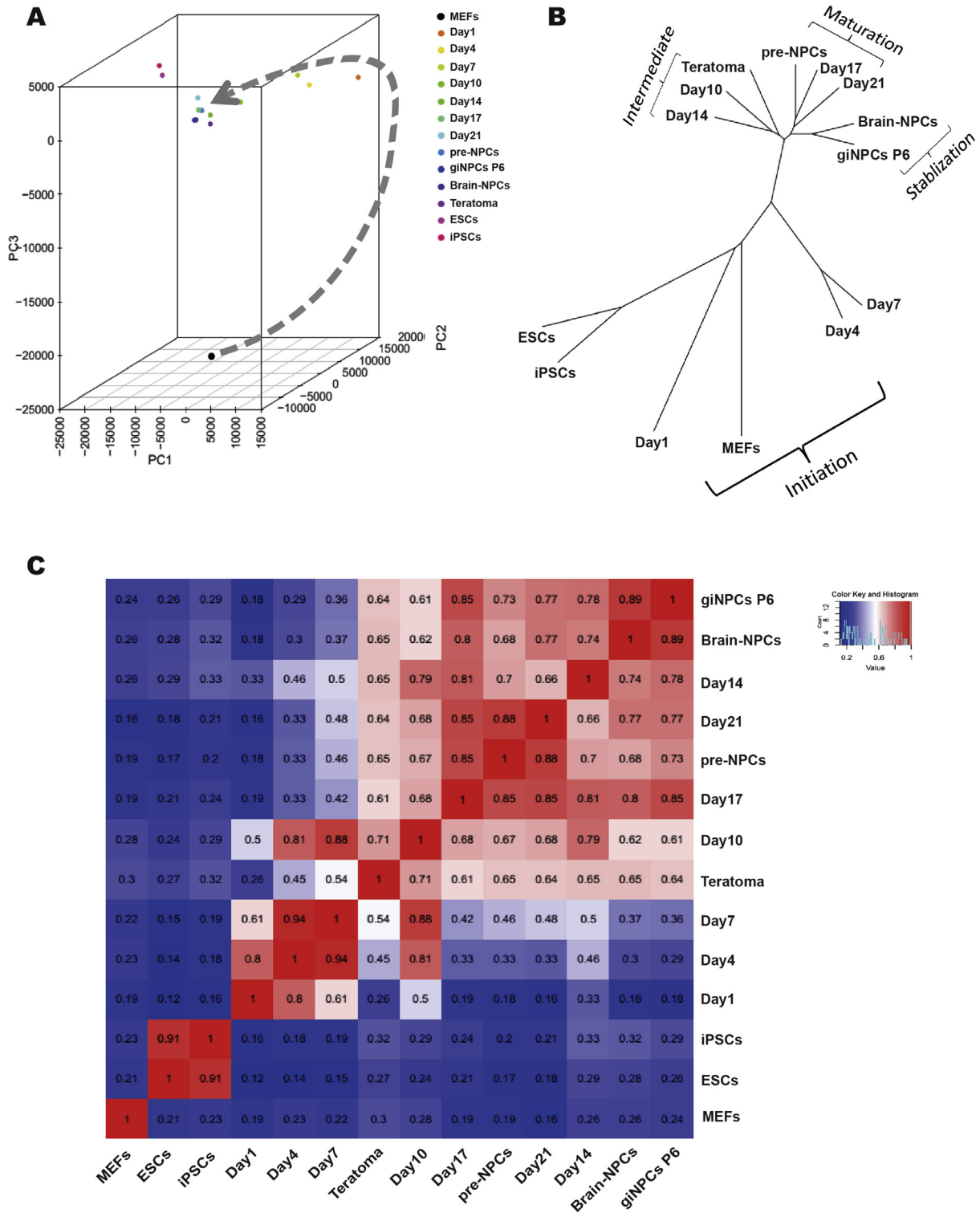

Fig. 5. Induction from MEFs into giNPCs is a gradual process. (A) Three-dimensional principal component analysis (PCA) of gene expression in cell samples during the giNPC induction process at indicated time points. Sequencing reads of MEFs (GSE43986), mouse ESCs (GSE59463) and iPSCs (GSE54619) are cited from public datasets. The arrow indicates a gradual induction process from the MEF state to the NPC state. (B) Unsupervised hierarchical clustering of gene expression profiles clearly shows that the giNPC induction process goes through four stages. (C) Hierarchical clustering and Pearson correlation analysis of different time points during the giNPC induction process. The color represents the Pearson correlation coefficient (red for higher correlation and blue for lower correlation), and the values are indicated. (For interpretation of the references to colour in this figure legend, the reader is referred to the web version of this article.)

as *Pax6*, *Sox2* as well as *Nestin*, were gradually reactivated from the intermediate stage and highly expressed in the maturation and stabilization stages (Fig. 6A, clusters V, VI and VII and Fig. 6B–C). Additionally, expression of brain region-specific genes, including ventral brain-specific markers (such as *Olig2*), dorsal brain markers (such as *Sox3*), forebrain markers (such as *Foxg1*), midbrain markers

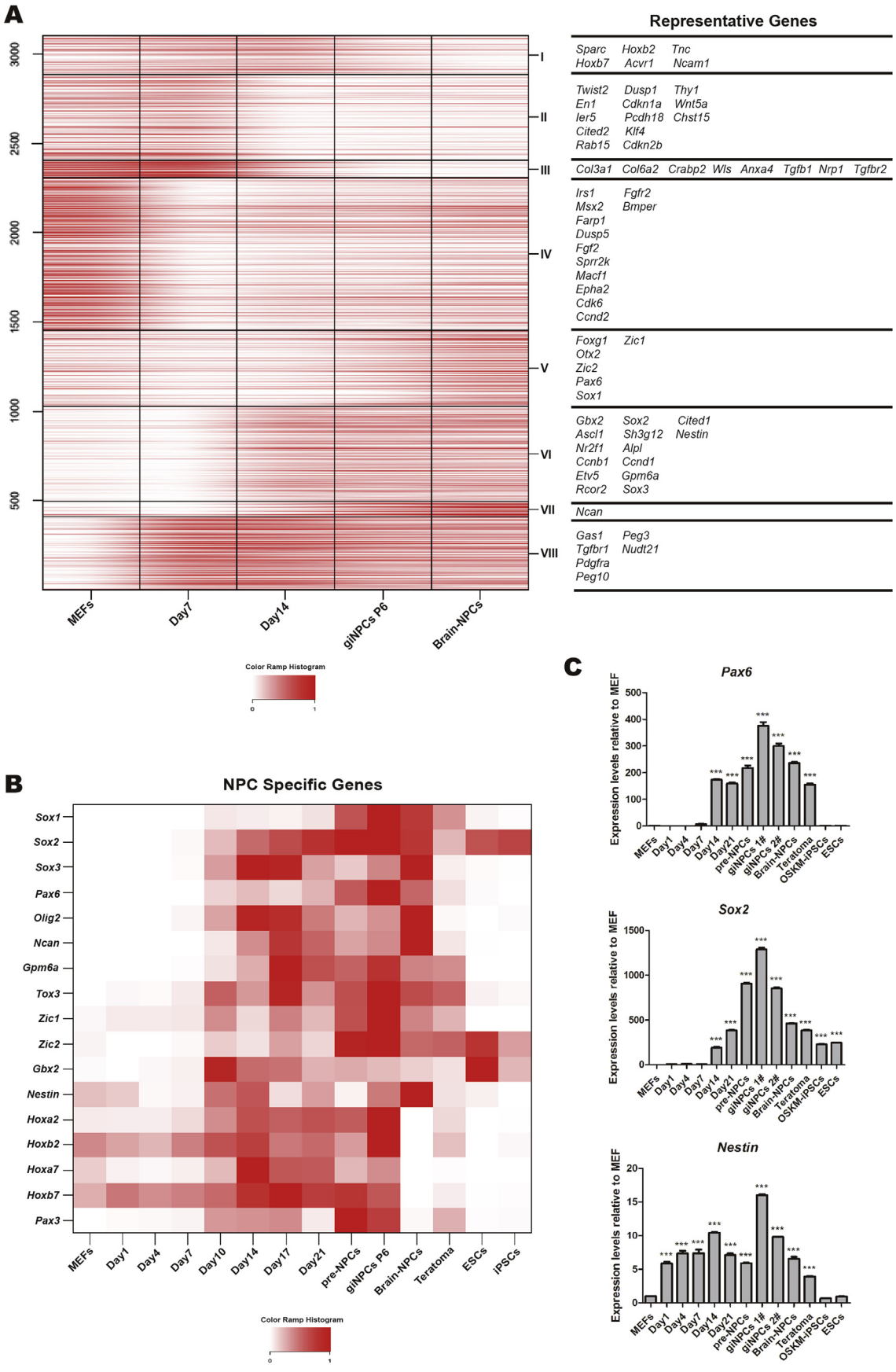

Fig. 6. Transcriptome dynamics in the direct induction system. (A) Clustering of gene-expression profiles based on transcriptome dynamics during the giNPC induction process. The genes were clustered into eight groups (I–VIII), according to the expression level using *k*-means algorithms. Each row is a gene (representative genes are listed in the right panel), and each column represents a sample. The gene-expression intensity was scaled across samples (red for high expression and white for low expression). (B) Heatmap analysis showing dynamic changes of NPC specific and brain region-specific genes during the giNPC induction process. (C) qRT-PCR validation of NPC markers during the giNPC induction process. The expression levels are normalized to those observed in MEFs. Data in (C) are represented as the mean ± SEM (n = 3). ***p < 0.001 by ANOVA or Student's *t*-test for comparison. (For interpretation of the references to colour in this figure legend, the reader is referred to the web version of this article.)

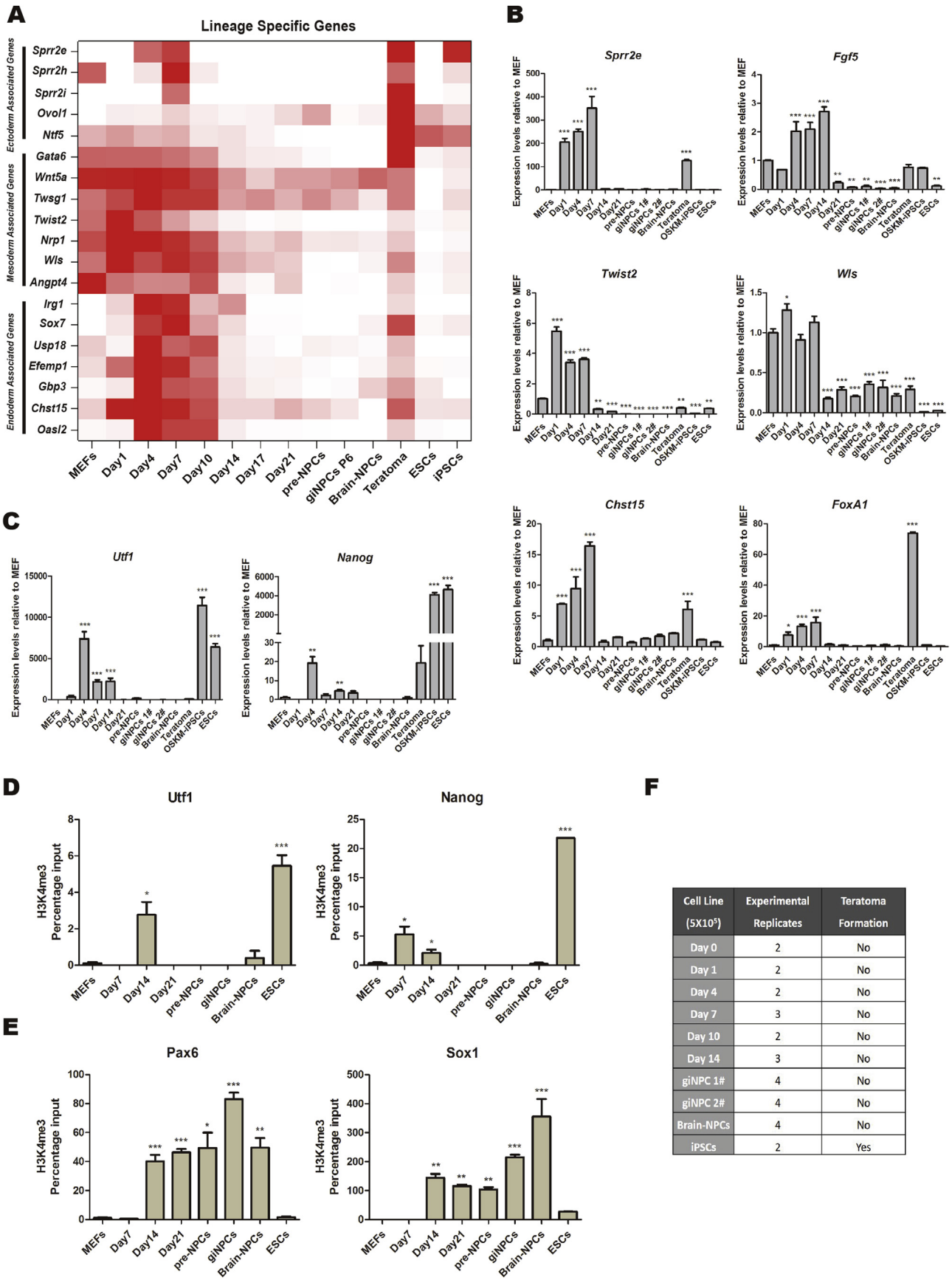

Cell Line ($5X10^5$)	Experimental Replicates	Teratoma Formation
Day 0	2	No
Day 1	2	No
Day 4	2	No
Day 7	3	No
Day 10	2	No
Day 14	3	No
giNPC 1#	4	No
giNPC 2#	4	No
Brain-NPCs	4	No
iPSCs	2	Yes

Fig. 7. Direct induction undergoes a transient partially reprogrammed state. (A) Dynamic changes of lineage-specific (ectoderm-, mesoderm- and endoderm-) genes during the giNPC induction process presented by heatmap analysis. Lineage specific genes were up-regulated in the first 2-weeks. (B) qRT-PCR analysis of indicated lineage-specific genes

(such as *Gbx2* and *En1*) and posterior brain markers (such as *Hoxb7*), were also up-regulated during this process and maintained in giNPCs (Fig. 6B). Together, these data suggest that induction of MEFs into giNPCs is a gradual process that occurs by removal of somatic structure (Fig. 5A–B, 6A and S4B) and establishment of an NPC specific network (Fig. 5A–B and 6A-B). Moreover, similar processes were also observed both in the fibroblast-giNPC induction (Fig. S5A and S5B) and in the recently reported ciNPC induction system (Fig. S5C–5F).

3.7. Direct induction undergoes a transient partially reprogrammed state

To better understand how the transgene-free iNPC network was set up, we sought insight into the molecular mechanism of the entire induction process. Using PCA and unsupervised hierarchical clustering analyses, we noticed a particular period in which cells showed a transient partially reprogrammed transcriptional platform and presented a transcriptome similar to that of teratomas, which are known to express genes from three germ layers (Fig. 5A–B and 7A). Specifically, several lineage specific (ectoderm-, mesoderm- and endoderm-) genes were up-regulated at the initiation stage from Day 1 and maintained relatively high expression levels for about two weeks until the maturation stage (Fig. 7A). Moreover, qRT-PCR analysis demonstrated that ectoderm associated genes (*Sprr2e*, *Fgf5* and *Sprr2i*), mesoderm associated genes (*Twist2* and *Wls*) and endoderm associated genes (*Chst15*, *FoxA1*, *Afp* and *Sox17*) were up-regulated from Day 1 to Day 7 and were down-regulated thereafter (Fig. 7B and S6A). Interestingly, the fibroblast-giNPC induction process as well as the ciNPC induction system also showed a similar transcriptional tendency of these lineage specific genes (Fig. S7A, S8A and S9A). Surprisingly, we noticed that certain core pluripotent transcription factors, such as *Utf1*, *Nanog*, *Oct4*, *Rex1*, *Dppa4* and *Fgf4* (Fig. 7C and S6B), were transiently up-regulated in giNPC induction. Moreover, the up-regulation of core pluripotent genes was also noticed in fibroblast-giNPC and ciNPC system (Fig. S7B, S8B and S9B). In addition, chromatin immunoprecipitation analysis indicated that promoters of Utf1 and Nanog underwent a transient burst of activating H3K4 trimethylation and a concomitant down-regulation of repressive H3K27me3 marks during the giNPC induction both from MEFs (Fig. 7D and S6C) and fibroblasts (Fig. S7C and S7E). Importantly, despite a relatively low level, these histone modification changes at the pluripotent promoters had a pattern similar to that of mouse ESCs, which further indicated that giNPC induction undergoes a transient partially reprogrammed state. In contrast, the promoter regions of Pax6 and Sox1 gradually gained H3K4 trimethylation and reduced H3K27 trimethylation from Day 14 onward, respectively (Fig. 7E, S6D, S7D and S7F).

As the cells during the giNPC induction process showed a transient partially reprogrammed state, the tumorigenicity of these cells deserves our concern. Thus, teratoma formation assay was further performed to test the potential tumorigenic ability of these cells as well as the established giNPCs. When subcutaneously injected into immune-deficient mice, neither these partially reprogrammed cells nor giNPCs could generate any teratomas, which was quite similar to Brain-NPCs (Fig. 7F and S10A-S10C). As positive controls, iPS cells were capable of forming the teratoma with derivatives from all three germ layers (Fig. 7F and S10B).

Collectively, these results strongly support the notion that direct induced mouse NPCs undergo a partially reprogrammed state, during which certain lineage specific and pluripotency associated genes will be transiently activated, whereas NPC specific markers are gradually up-regulated. Then, the fully induced NPCs were established.

4. Discussion

Generation of desirable functional cells holds great potential for both research and clinical applications. Recently, several effective strategies have been developed to obtain neural cells and neural progenitor cells, which, in the future, may help treat the selective dysfunctional neurons in most neurodegenerative disorders [2,3,5,8–12]. Thus, it is important to understand technical and functional advantages and disadvantages as well as the underlying molecular mechanism of such methods. Although functional NPCs could be efficiently derived from embryonic stem cells (ESCs) and induced pluripotent stem cells (iPSCs) [2,9–12], the ethical issues of ESCs and the risk of tumorigenesis observed in iPSCs limit their use in clinical treatment. Similarly, the low yield of neurons generated by the direct reprogramming approach also restricts their further use [5,8]. Thus, the direct conversion of somatic cells into multipotent and lineage-restricted NPCs is highly desirable. Although the overexpression of master transcription factors is considered the major determinant of cellular fate conversion, transdifferentiation mediated by small molecules has great advantages, including non-immunogenicity and non-transgene integration, despite that the underlying mechanism remains elusive [25,26,42–45].

Ectopic expression of the NPC-related factors or transient expression of pluripotent-related factors with neural-lineage signals during NPC conversion from fibroblasts would direct the exogenous factors to recognize specific loci and recruit and/or cooperate with other endogenous regulators to establish a NPC identity [17–21,23,24]. Meanwhile, small molecules that have the ability to activate neuro-lineage signaling or modulate epigenetic modifications also help for the NPC conversion [25,26]. However, the same situation is that both methods break the original steady somatic state by exogenous substances (exogenous transcription factors or small molecules) and then activating endogenous neural related transcription factors and/or signaling pathways [17–20,23–26]. Accordingly, we hypothesized that external inductive and/or permissive signaling conditions might also have the same potential. Based on this speculation, we established a novel growth factor based culture system and successfully used it to achieve a direct lineage conversion by inducing somatic cells into functional neural progenitor cells (giNPCs) in the present study (Fig. 1 and 3). These giNPCs exhibited similar morphological and molecular features as well as transcriptional network to those of neonatal mouse brain–derived NPCs, but were quite different from the starting cells (Fig. 1B, 2, 3 and S2). Notably, these giNPCs maintained their characteristics over prolonged expansion (>20 passages) (Fig. 2D–E and S2E-S2F) and could give rise to major neural lineages *in vivo* and *in vitro* (Fig. 4 and S3). Thus, in conclusion, the giNPCs showed typical features of Brain-NPCs,

(ectoderm associated genes-*Sprr2e* and *Fgf5*, mesoderm associated genes-*Twist2* and *Wls* as well as endoderm associated genes-*Chst15* and *FoxA1*) during the giNPC induction process. The expression levels were normalized to those observed in MEFs. (C) qRT-PCR analysis of pluripotent genes during the giNPC induction process. The expression levels were normalized to those observed in MEFs. (D–E) Time course analysis of histone modification during the giNPC induction process. Utf1 and Nanog promoter loci (D) and Pax6 and Sox1 promoter loci (E) were analyzed by chromatin immunoprecipitation with antibodies against the epigenetic marks H3K4me3 during this process. The data are percentages of the input chromatin amount, analyzed by qPCR. (F) Table summarizing the teratoma formation ability of indicated cells. Briefly, the induction of cells from Day 0, Day 1, Day 4, Day 7, Day 10, and Day 14 as well as giNPC lines 1# and 2# could not generate teratomas in immune-deficient mice within 1 months' observation. iPSCs were set as the positive control. Data in (B)–(E) are represented as the mean ± SEM (n = 3). *p < 0.05; **p < 0.01; ***p < 0.001 by ANOVA or Student's *t*-test for comparison.

which are self-renewal and neural multipotent.

We have also tested whether human fibroblasts can be induced into NPCs by this growth factor mediated method. When human fibroblast cells were induced by the same procedures, compact cell colonies resembling those obtained in growth factor treated mouse cells could emerge after 30 days (data not shown). However, despite that they show similar morphologies to that of mouse NPCs, these human fibroblasts derived colonies cannot efficiently up-regulate NPC-specific genes. Thus, these results indicated that the growth factors in current protocol may not be enough to activate endogenous genes in human system. Therefore, this strategy should be further optimized to obtain human giNPCs.

Because induced pluripotency is established in a step-wise manner, previous studies hypothesized that brief reactivation of reprogramming factors in somatic cells would generate a highly plastic intermediate state (Oct4-GFP negative) instead of a mature iPSC state (Oct4-GFP positive), and that, thereafter, the induced cells could further differentiate into different lineages under certain inductive signals [17,29]. However, recent findings from two groups refuted this argument and demonstrated that pluripotency-associated transcription factor mediated lineage conversion involves a transient passage through an iPSC stage [31,32]. As the analyses conducted in previous studies were based on ectopic transgene mediated transdifferentiation, the understanding of the molecular mechanisms underlying transgene-free iNPC generation remains elusive. In the present study, we demonstrated that both our growth factor-induced and recently reported chemical-induced NPC undergo a gradual induction process that included the removal of somatic structure and the establishment of an NPC specific network, which typically includes initiation, intermediate, maturation and stabilization stages (Fig. 5A–B, 6B-C, S4B-S4C and S5). Most importantly, we noticed a special period in this growth factor mediated lineage conversion process, during which cells showed a transient partially reprogrammed transcriptional platform and activated not only genes from the three germ layers (Fig. 5A–B, 7A-B, S6A and S7A) but also pluripotent genes (Fig. 7C, S6B and S7B) to a certain extent. The induction of a developmental open-chromatin state was further marked by a transient burst of activating H3K4 trimethylation (Fig. 7D and S7C) and a contaminant down-regulation of repressive H3K27me3 marks (Fig. S6C and S7E) within the promoters of Utf1 and Nanog. Moreover, a similar transient up-regulation of lineage specific genes as well as pluripotent genes was also noticed in the previously reported chemical based means (Fig. S8 and S9) [25]. Although those partially reprogrammed cells did not contribute to teratomas in immune-deficient mice, we still could not ignore potential safety concerns (Fig. 7F and S10). Thus, a more in-depth understanding of fully- and partially-reprogrammed stages is required to provide safety verification information for generating functionally desirable cell types for potential regenerative applications in the future.

5. Conclusion

In summary, we describe a novel method for generating growth factor-induced neural progenitor cells (giNPCs) by using inductive and permissive signaling culture conditions with the combination of only a few growth factors. Thus, ours and other recent studies [25,26,42–44] provide evidence that direct lineage-specific conversion can be achieved without introducing ectopic transcriptional factors. Importantly, we demonstrate that the direct cell type switch from somatic cells (both MEFs and adult fibroblasts) to functional NPCs by growth factors or small molecules both go through a transient partially reprogrammed state. Our study therefore highlights the importance of excluding the possibility of residual partially reprogrammed or teratoma-like cells in the transgene-free direct induction strategy for future clinical trials.

Author contributions

R.G. and W.X.: conception and design, collection and/or assembly of data, data analysis and interpretation and manuscript writing. L.Z., R.Z., L.Y., C.W., M.W., M. W., L.Y., Y.T., Y. G., H.W., J.X., W.L., Y.W., X.W., Y.Y. and Y.Z.: provision of study materials and data analysis and interpretation. J.C., L.C. and S.G.: conception and design, financial support, data analysis and interpretation, manuscript writing and final approval of the manuscript.

Acknowledgements

We are grateful to our colleagues in the laboratory for their assistance with the experiments and in the preparation of this manuscript. We thank Prof. Yuqiang Ding for sharing the Nestin-GFP transgenic mice. This project was supported by the National Natural Science Foundation of China (31401247, 31401266, 31325019, 91319306, 31471392, 31430056 and 31501196), the Ministry of Science and Technology of China (grants 2014CB964601, 2015CB964503, 2016YFA0100400 and 2015CB964800), the Science and Technology Commission of Shanghai Municipality (YF1403900), the Shanghai Municipal Education Commission (14CG16) and the Program for Young Excellent Talents in Tongji University (grants 2000219115, 2000219117 and 1515219023).

Appendix A. Supplementary data

Supplementary data related to this article can be found at http://dx.doi.org/10.1016/j.biomaterials.2016.12.007.

References

[1] K. Takahashi, K. Tanabe, M. Ohnuki, M. Narita, T. Ichisaka, K. Tomoda, et al., Induction of pluripotent stem cells from adult human fibroblasts by defined factors, Cell 131 (2007) 861–872.
[2] I.H. Park, N. Arora, H. Huo, N. Maherali, T. Ahfeldt, A. Shimamura, et al., Disease-specific induced pluripotent stem cells, Cell 134 (2008) 877–886.
[3] F. Soldner, D. Hockemeyer, C. Beard, Q. Gao, G.W. Bell, E.G. Cook, et al., Parkinson's disease patient-derived induced pluripotent stem cells free of viral reprogramming factors, Cell 136 (2009) 964–977.
[4] Z.P.P. Pang, N. Yang, T. Vierbuchen, A. Ostermeier, D.R. Fuentes, T.Q. Yang, et al., Induction of human neuronal cells by defined transcription factors, Nature 476 (2011). 220-U122.
[5] L. Qiang, R. Fujita, T. Yamashita, S. Angulo, H. Rhinn, D. Rhee, et al., Directed conversion of Alzheimer's disease patient skin fibroblasts into functional neurons, Cell 146 (2011) 359–371.
[6] M. Caiazzo, M.T. Dell'Anno, E. Dvoretskova, D. Lazarevic, S. Taverna, D. Leo, et al., Direct generation of functional dopaminergic neurons from mouse and human fibroblasts, Nature 476 (2011). 224-U151.
[7] E.Y. Son, J.K. Ichida, B.J. Wainger, J.S. Toma, V.F. Rafuse, C.J. Woolf, et al., Conversion of mouse and human fibroblasts into functional spinal motor neurons, Cell Stem Cell 9 (2011) 205–218.
[8] J. Jiao, Y.Y. Yang, Y.W. Shi, J.Y. Chen, R. Gao, Y. Fan, et al., Modeling Dravet syndrome using induced pluripotent stem cells (iPSCs) and directly converted neurons, Hum. Mol. Genet. 22 (2013) 4241–4252.
[9] T. Yagi, D. Ito, Y. Okada, W. Akamatsu, Y. Nihei, T. Yoshizaki, et al., Modeling familial Alzheimer's disease with induced pluripotent stem cells, Hum. Mol. Genet. 20 (2011) 4530–4539.
[10] K.J. Brennand, A. Simone, J. Jou, C. Gelboin-Burkhart, N. Tran, S. Sangar, et al., Modelling schizophrenia using human induced pluripotent stem cells, Nature 473 (2011) 221.
[11] M.A. Israel, S.H. Yuan, C. Bardy, S.M. Reyna, Y.L. Mu, C. Herrera, et al., Probing sporadic and familial Alzheimer's disease using induced pluripotent stem cells, Nature 482 (2012). 216-U107.
[12] M.C.N. Marchetto, C. Carromeu, A. Acab, D. Yu, G.W. Yeo, Y.L. Mu, et al., A model for neural development and treatment of Rett syndrome using human induced pluripotent stem cells, Cell 143 (2010) 527–539.
[13] M. Wernig, A. Meissner, J.P. Cassady, R. Jaenisch, c-Myc is dispensable for direct reprogramming of mouse fibroblasts, Cell Stem Cell 2 (2008) 10–12.
[14] J.Y. Chen, Y.W. Gao, H. Huang, K. Xu, X.H. Chen, Y.H. Jiang, et al., The combination of Tet1 with Oct4 generates high-quality mouse-induced pluripotent stem cells, Stem Cells 33 (2015) 686–698.

[15] G. Martino, S. Pluchino, The therapeutic potential of neural stem cells, Nat. Rev. Neurosci. 7 (2006) 395–406.
[16] P. Taupin, The therapeutic potential of adult neural stem cells, Curr. Opin. Mol. Ther. 8 (2006) 225–231.
[17] J. Kim, J.A. Efe, S.Y. Zhu, M. Talantova, X. Yuan, S.F. Wang, et al., Direct reprogramming of mouse fibroblasts to neural progenitors, Proc. Natl. Acad. Sci. U. S. A. 108 (2011) 7838–7843.
[18] E. Lujan, S. Chanda, H. Ahlenius, T.C. Sudhof, M. Wernig, Direct conversion of mouse fibroblasts to self-renewing, tripotent neural precursor cells, Proc. Natl. Acad. Sci. U. S. A. 109 (2012) 2527–2532.
[19] M. Thier, P. Worsdorfer, Y.B. Lakes, R. Gorris, S. Herms, T. Opitz, et al., Direct conversion of fibroblasts into stably expandable neural stem cells, Cell Stem Cell 10 (2012) 473–479.
[20] D.W. Han, N. Tapia, A. Hermann, K. Hemmer, S. Hoing, M.J. Arauzo-Bravo, et al., Direct reprogramming of fibroblasts into neural stem cells by defined factors, Cell Stem Cell 10 (2012) 465–472.
[21] C. Sheng, Q.Y. Zheng, J.Y. Wu, Z. Xu, L.B. Wang, W. Li, et al., Direct reprogramming of Sertoli cells into multipotent neural stem cells by defined factors, Cell Res. 22 (2012) 208–218.
[22] J.P. Cassady, A.C. D'Alessio, S. Sarkar, V.S. Dani, Z.P. Fan, K. Ganz, et al., Direct lineage conversion of adult mouse liver cells and B lymphocytes to neural stem cells, Stem Cell Rep. 3 (2014) 948–956.
[23] K.L. Ring, L.M. Tong, M.E. Balestra, R. Javier, Y. Andrews-Zwilling, G. Li, et al., Direct reprogramming of mouse and human fibroblasts into multipotent neural stem cells with a single factor, Cell Stem Cell 11 (2012) 100–109.
[24] L.H. Wang, L.L. Wang, W.H. Huang, H.X. Su, Y.T. Xue, Z.H. Su, et al., Generation of integration-free neural progenitor cells from cells in human urine, Nat. Methods 10 (2013) 84–U124.
[25] L. Cheng, W.X. Hu, B.L. Qiu, J. Zhao, Y.C. Yu, W.Q. Guan, et al., Generation of neural progenitor cells by chemical cocktails and hypoxia, Cell Res. 24 (2014) 665–679.
[26] M. Zhang, Y.H. Lin, Y.J. Sun, S. Zhu, J. Zheng, K. Liu, et al., Pharmacological reprogramming of fibroblasts into neural stem cells by signaling-directed transcriptional activation, Cell Stem Cell 18 (2016) 653–667.
[27] T. Graf, T. Enver, Forcing cells to change lineages, Nature 462 (2009) 587–594.
[28] T. Vierbuchen, M. Wernig, Direct lineage conversions: unnatural but useful? Nat. Biotechnol. 29 (2011) 892–907.
[29] J.A. Efe, S. Hilcove, J. Kim, H. Zhou, K. Ouyang, G. Wang, et al., Conversion of mouse fibroblasts into cardiomyocytes using a direct reprogramming strategy, Nat. Cell Biol. 13 (2011), 215-U61.
[30] S.Y. Zhu, M. Rezvani, J. Harbell, A.N. Mattis, A.R. Wolfe, L.Z. Benet, et al., Mouse liver repopulation with hepatocytes generated from human fibroblasts, Nature 508 (2014) 93–97.
[31] O. Bar-Nur, C. Verheul, A.G. Sommer, J. Brumbaugh, B.A. Schwarz, I. Lipchina, et al., Lineage conversion induced by pluripotency factors involves transient passage through an iPSC stage, Nat. Biotechnol. 33 (2015) 761–768.
[32] I. Maza, I. Caspi, A. Zviran, E. Chomsky, Y. Rais, S. Viukov, et al., Transient acquisition of pluripotency during somatic cell transdifferentiation with iPSC reprogramming factors, Nat. Biotechnol. 33 (2015) 769–774.
[33] A.D. Ebert, E.L. McMillan, C.N. Svendsen, Isolating, expanding, and infecting human and rodent fetal neural progenitor cells, Curr. Protoc. Stem Cell Biol. (2008 Sep), http://dx.doi.org/10.1002/9780470151808.sc02d02s6 (Chapter 2): Unit 2D.
[34] C.H. Tian, Q. Liu, K.M. Ma, Y.X. Wang, Q. Chen, R. Ambroz, et al., Characterization of induced neural progenitors from skin fibroblasts by a novel combination of defined factors, Sci. Rep. U. K. (2013) 3.
[35] Y.Y. Yang, J. Jiao, R. Gao, R.R. Le, X.C. Kou, Y.H. Zhao, et al., Enhanced rejuvenation in induced pluripotent stem cell-derived neurons compared with directly converted neurons from an aged mouse, Stem Cells Dev. 24 (2015) 2767–2777.
[36] L. Cheng, W.X. Hu, B.L. Qiu, J. Zhao, Y.C. Yu, W.Q. Guan, et al., Generation of neural progenitor cells by chemical cocktails and hypoxia (vol 24, pg 665, 2014), Cell Res. 25 (2015) 645–646.
[37] Y.C. Yu, S. He, S. Chen, Y. Fu, K.N. Brown, X.H. Yao, et al., Preferential electrical coupling regulates neocortical lineage-dependent microcircuit assembly, Nature 486 (2012) 113–117.
[38] C. Trapnell, L. Pachter, S.L. Salzberg, TopHat: discovering splice junctions with RNA-Seq, Bioinformatics 25 (2009) 1105–1111.
[39] C. Trapnell, B.A. Williams, G. Pertea, A. Mortazavi, G. Kwan, M.J. van Baren, et al., Transcript assembly and quantification by RNA-Seq reveals unannotated transcripts and isoform switching during cell differentiation, Nat. Biotechnol. 28 (2010) 511–515.
[40] M.D. Robinson, D.J. McCarthy, G.K. Smyth, edgeR: a Bioconductor package for differential expression analysis of digital gene expression data, Bioinformatics 26 (2010) 139–140.
[41] P. Samavarchi-Tehrani, A. Golipour, L. David, H.K. Sung, T.A. Beyer, A. Datti, et al., Functional genomics reveals a BMP-driven mesenchymal-to-epithelial transition in the initiation of somatic cell reprogramming, Cell Stem Cell 7 (2010) 64–77.
[42] X. Li, X.H. Zuo, J.Z. Jing, Y.T. Ma, J.M. Wang, D.F. Liu, et al., Small-molecule-driven direct reprogramming of mouse fibroblasts into functional neurons, Cell Stem Cell 17 (2015) 195–203.
[43] W.X. Hu, B.L. Qiu, W.Q. Guan, Q.Y. Wang, M. Wang, W. Li, et al., Direct conversion of normal and Alzheimer's disease human fibroblasts into neuronal cells by small molecules, Cell Stem Cell 17 (2015) 204–212.
[44] Y.B. Fu, C.W. Huang, X.X. Xu, H.F. Gu, Y.Q. Ye, C.Z. Jiang, et al., Direct reprogramming of mouse fibroblasts into cardiomyocytes with chemical cocktails, Cell Res. 25 (2015) 1013–1024.
[45] J. Xu, Y.Y. Du, H.K. Deng, Direct lineage reprogramming: strategies, mechanisms, and applications, Cell Stem Cell 16 (2015) 119–134.